Fitting Medium and High Degrees using GONG, MDI and HMI Observations.

S.G. Korzennik
Harvard-Smithsonian Center for Astrophysics, Cambridge, MA

Medium Degrees

- Fit all available data since 1995, using my state of the art fitting methodology.

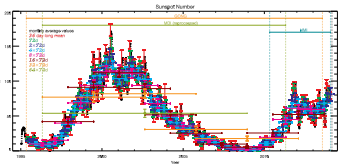

Fig. 1: *Activity index, i.e., sunspot number, over the past 19 years and its mean value for the different fitted epochs.*

Changes in Mode Parameters with Activity

- Frequency

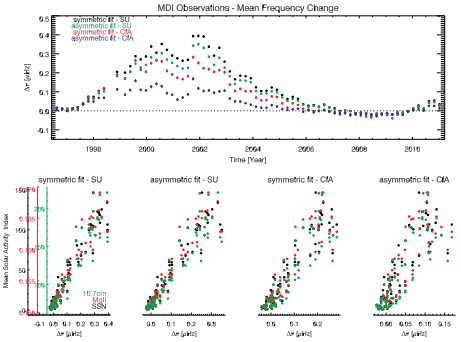

Fig. 2: *Top panel: mean frequency change with respect to epoch, when fitting MDI observations using symmetric or asymmetric fits, produced by the MDI project (SU) or by my own independent fitting (CfA). Bottom panels: the mean changes compared to three solar activity indices.*

- FWHM, Γ and Asymmetry, α

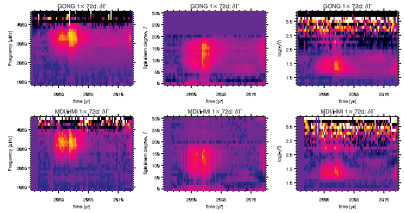

Fig. 3: *Change in FWHM, Γ as a function of epoch –hence solar activity– and ν, ℓ, or $\log(\nu/L)$ (left to right). The top row shows results from fitting GONG observations, the bottom row from fitting MDI observations.*

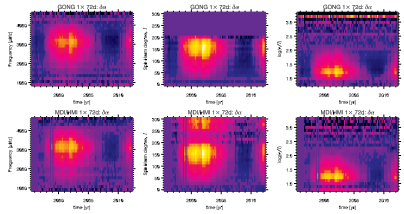

Fig. 4: *Change in asymmetry, α, as a function of epoch –hence solar activity– and ν, ℓ, or $\log(\nu/L)$ (left to right). The top row shows results from fitting GONG observations, the bottom row from fitting MDI observations.*

Changes in Solar Rotation with Activity

- Residual Rotation (AKA Torsional Oscillations)

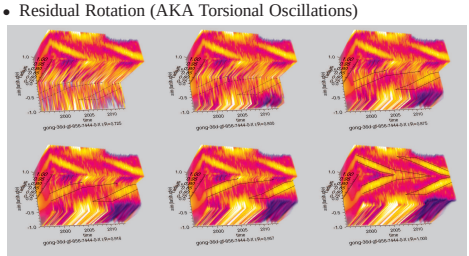

Fig. 5: *Rotation rate in the top 28.7% of the solar interior (the convection zone), as a function of time, latitude and depth, after subtracting the mean rotation profile for Cycle 23. Each panel shows a cut of the residual rate at a given depth, and the outline of the surface torsional oscillation (*faster than the mean *outline).*

- Comparison of Cycle 23 to Cycle 24

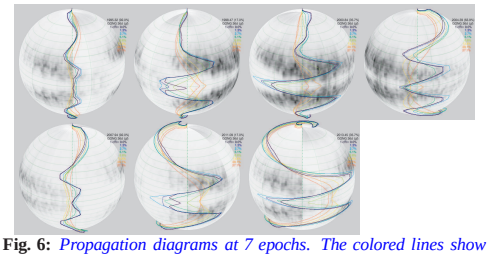

Fig. 6: *Propagation diagrams at 7 epochs. The colored lines show the torsional displacement with respect to the mean rotation profile at 8 depths throughout the convection zone. A rotating butterfly diagram is wrapped onto the sphere. The top row shows the end of Cycle 22 and Cycle 23, the bottom row shows equivalent epochs as the top row but for the end of Cycle 23 and for Cycle 24. The propagation diagrams in the bottom row shows clearly that the signature of the torsional oscillations is stronger during Cycle 24 than Cycle 23 (robust) and that the rotation rate in the lower part of the convection zone during Cycle 24 has a different equatorial component than during Cycle 23 (weaker result).*

High Degrees

- Analyzed five data sets (3 instruments and 3 co-eval epochs).

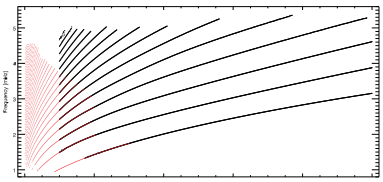

Fig. 7: *Coverage in the (ℓ, ν) plane of inverted data sets: low and intermediate degrees, derived from fitting resolved modes, are shown in red, the high degrees modes, derived from ridge fitting, are shown as the larger black circles.*

Year	Instrument	$\Delta\nu$	$\Delta\nu/\sigma_\nu$
2001	MDI	-0.220 ± 0.673	-0.880 ± 2.182
2002	MDI	-0.298 ± 0.966	-0.862 ± 2.631
	GONG	0.176 ± 0.769	0.517 ± 2.416
2010	MDI	-0.088 ± 1.087	-0.077 ± 2.766
	GONG	0.748 ± 1.186	2.751 ± 2.411
	HMI	0.269 ± 0.616	0.880 ± 2.044

Table 1: *Mean and standard deviation of frequency differences, and scaled frequency differences, between estimated mode frequencies derived from ridge fitting and co-eval resolved mode frequencies measurements, for the $100 \le \ell \le 200|300$ overlapping range.*

Year	Instruments	$\Delta\nu$	$\Delta\nu/\sigma_\nu$
2002	GONG – MDI	-0.222 ± 0.460	-1.317 ± 1.470
2010	GONG – MDI	-0.982 ± 0.934	-4.260 ± 2.770
	HMI – MDI	-0.655 ± 1.117	-2.162 ± 1.572

Table 2: *Mean and standard deviation of frequency differences, and scaled frequency differences, between estimated mode frequencies derived from ridge fitting for different instruments and co-eval epochs, with respect to MDI values.*

Rotational Splittings

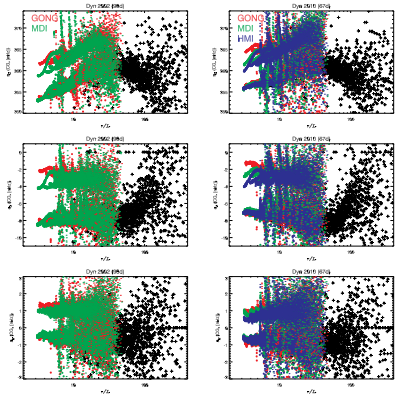

Fig. 8: *Comparison of Clebsch–Gordan rotational frequency splitting coefficients.Panels on the left compare 2002 results, on the right 2010 results. Colored dots correspond to the ridge frequencies, colored circles to mode frequency estimates (i.e., after correction).Black crosses are values obtained by fitting resolved modes.*

Solar Rotation

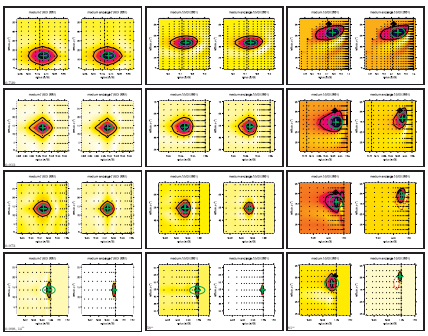

Fig. 9: *Averaging kernels, at 3 latitudes and 4 depths, corresponding to rotation inversions using or not high degree modes (left vs right panels within each box). The target locations are indicated by the black cross-diamond symbols, the green crosses and circles illustrate the kernel center of gravity and width estimate. The black dots delineate the inversion grid. The half height contours of the averaging kernels resulting from inverting the medium degrees are overlapped in red on the corresponding averaging kernel computed for the medium and high degree case.*

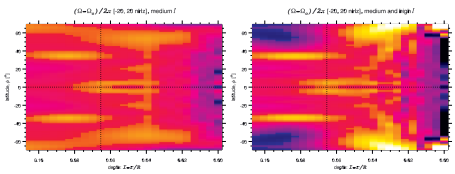

Fig. 10: *Rotation rate in the outer 10% of the solar interior, as a function of depth and latitude, after subtracting a differential rotation profile, inferred using or not high degree modes (right and left panels respectively). Note how (a) the "torsional oscillations" signal stands out more clearly in the bottom half of the outer 10% when including high degrees, and (b) the profiles are quite different in the top 5%, especially at high latitudes.*

Conclusions

Medium Degrees – ($0 \le \ell \le 300$)

- Different signature of $\Delta\nu$ when including asymmetry
- FWHM and Asymmetry change with activity
- Torsional oscillations:
  - ▹ penetrate down to $\approx 0.875\, r/R_\odot$
  - ▹ migrate to lower latitudes at larger depths
- Solar Rotation during Cycle 24 *is* different from Cycle 23

High Degrees – ($100 \le \ell \le 1000$)

- High-ℓ mode characteristics using MDI, GONG & HMI.
- Good validation of corrected multiplets ($100 \le \ell \le 200|300$).
- Good agreement between instruments for co-eval epochs, but
  - ▹ frequency mismatch at higher degrees,
  - ▹ corrected rotational splittings agree a lot better than the raw (ridge) values (validation).
- Limiting factor is likely to be PSF.
- Inclusion of high degree splittings for rotation inversions:
  - ▹ improve resolution kernels close to surface (high latitudes)
  - ▹ affect the results in the top 10%, and more so in the top 5%

Acknowledgments

The Solar Oscillations Investigation - Michelson Doppler Imager project on SOHO is supported by NASA grant NNX09AI90G at Stanford University. SOHO is a project of international cooperation between ESA and NASA. This work utilizes data obtained by the Global Oscillation Network Group (GONG) program, managed by the National Solar Observatory, which is operated by AURA, Inc. under a cooperative agreement with the National Science Foundation. HMI data courtesy of NASA and the HMI consortium; HMI is supported by NASA contract NAS5–02139 to Stanford University. SGK was supported by Stanford contract PR–6333 and NASA grants NAG5–9819 and NNG05GD58G.